minerals

MDPI

Article

Experimental Study on Cemented Filling of Granular Pile in Caving Goaf: A Case Study

Zhifu Dong [1,2], Jing Zhang [2,*], Fuqiang Ren [2] and Fengyu Ren [3]

[1] Yunnan Gold Mining Group Co., Ltd., Kunming 650299, China; dongzhifu1184@stu.kust.edu.cn
[2] Faculty of Land Resource Engineering, Kunming University of Science and Technology, Kunming 650093, China; 20242201152@stu.kust.edu.cn
[3] Department of Resources and Civil Engineering, Northeastern University, Shenyang 110819, China; renfengyu@mail.neu.edu.cn
* Correspondence: yuanzhongni33@163.com

Abstract

For the metal deposits exploited by the open-stope subsequent filling method, the goaf roof is prone to large-scale caving when the stope ore is not fully mined. This further results in the accumulation of a thick layer of waste rock on the goaf floor due to the caving of surrounding rocks. In the treatment using cemented filling, it is essential to ensure that the filling slurry fully permeates into the granular pile, and that the granular-cemented backfill possesses sufficient strength to guarantee the production safety of adjacent stopes. Taking the caving goaf of Shirengou Iron Mine as the engineering background, the effects of slurry concentration, cement–tailing ratio, height of the granular pile, and particle size of the granular rock on seepage laws are investigated by means of a self-developed simplified filling test device. The filling slurry concentration that meets the on-site requirements for fluidity and permeability is thereby determined. Meanwhile, by prefabricating the granular-cemented backfill, the characteristics of the self-supporting capacity and strength of the backfill are studied, considering factors such as different slurry concentrations, cement–tailing ratios, and curing ages. The results indicate that the cement–tailing ratio exerts the least influence on the seepage law, yet it has the most significant impact on the strength of the granular-cemented backfill. When the cement–tailing ratio of the filling slurry ranges from 1:8 to 1:4 with a concentration of 68%, the filling slurry can completely seep and cement the waste rock layer. At this point, the granular-cemented backfill strength can reach 1~2 MPa, which satisfies the seepage and cementation requirements for the waste rock inside the caving goaf of Shirengou Iron Mine.

Keywords: caving goaf; cemented filling; granular pile; seepage law; strength characteristic

Check for updates

Academic Editor: Elsabe Kearsley

Received: 5 December 2025
Revised: 19 January 2026
Accepted: 4 February 2026
Published: 5 February 2026

Copyright: © 2026 by the authors. Licensee MDPI, Basel, Switzerland. This article is an open access article distributed under the terms and conditions of the Creative Commons Attribution (CC BY) license.

1. Introduction

Filling mining serves as a core technical approach for green, safe, efficient, and low-carbon mine production [1–3], and exhibits significant practical value in ensuring underground mining safety and controlling surface rock movement [4,5]. Currently, the prevalent filling methods in metal mines include cemented filling [6], paste filling [7–9], and waste rock filling [10,11]. To achieve resource utilization of solid waste [12,13], most scholars have dedicated their work to investigating combined filling modes such as waste rock-cemented filling [14–16] and waste rock-paste filling [17,18], thereby further promoting the coordinated development of the mining area ecological environment and safe ore deposit mining.

The primary material for waste rock filling is derived from the waste rock generated during underground excavation. Characterized by the lowest production cost, it stands as one of the conventional filling methods in the early stage of filling mining applications. Ren et al. [19] adopted the waste rock concrete roof-contacting filling technology to eliminate goaf hazards adjacent to the main shaft of a fluorite mine; He et al. [20] implemented the large-scale mechanized solid waste filling for the super-large goaf of a mine, which effectively addressed the stability issue of super-large goafs.

However, due to constraints on waste rock storage space and filling transportation routes, relatively few mines rely entirely on waste rock for stope filling. Consequently, most scholars have focused on combining waste rock with other filling methods; specifically, by adjusting the particle size of waste rock, it can be preprocessed into aggregates for pipeline-transportable filling slurry [21]. In terms of slurry fluidity, Jin et al. [22] identified that fly ash enhances the flowability, filling ability, and mechanical strength of cement-fly ash tailings grouts, and clarified the underlying enhancement mechanism. To explore factors influencing the microstructure of waste rock backfill, Qiu et al. [23] examined the coupled effects of waste rock-to-tailings ratio and curing temperature on the pore structure and mechanical properties of cemented tailings–waste rock backfill, and proposed that the complexity of micropore structure is a key indicator of structural refinement. Regarding the strength of waste rock backfill, Gao et al. [24] and Zhang et al. [10] indicated that incorporating an appropriate amount of waste rock improves the initial stiffness, flexural strength, and modulus of backfill, with the optimal waste rock content and particle size being 40% and 4–6 mm, respectively. Gao et al. [25] further proposed that adding a suitable dosage of polypropylene fibers can enhance the strength of cementitious tailings–waste rock backfill. Chen et al. [26] revealed that with the increase in waste rock content, the fluidity of filling slurry first increases and then decreases, the bleeding rate rises gradually, and the compressive strength of backfill exhibits a similar trend of initial increase followed by decrease.

Current research on combined backfilling using waste rock indicates that most scholars [27,28] have focused primarily on waste rock pretreatment to meet the stope backfilling requirements for surrounding rock stability. However, due to constraints imposed by engineering and hydrogeological conditions, some mines [4,29,30] are confronted with the risk of stope instability and caving, which in turn leads to substantial waste rock accumulation inside the stope as a result of surrounding rock caving. This scenario is prevalent in metal deposits exploited via the open-stope subsequent backfilling method, such as the Shirengou Iron Mine [4], Gangli Iron Mine [29] and the Zhongguan Iron Mine [30]. The primary cause of this issue lies in the well-developed joint fissures and poor stability of the stope roof surrounding rock. Before the full extraction of the stope, the surrounding rock of the goaf undergoes intense paroxysmal collapse, resulting in the formation of a thick waste rock layer at the goaf bottom. When backfilling measures are adopted for remediation under such circumstances, two critical requirements must be satisfied: first, the backfill slurry must maintain adequate fluidity [31] within the waste rock aggregate; second, the backfill body, after seepage and cementation, must exhibit sufficient strength [32] to ensure the production safety of adjacent stopes. This presents new challenges for addressing practical engineering problems of this type.

In the following sections, this study takes the caving goaf with the "backfilling-while-caving" characteristic in the Shirengou Iron Mine as the engineering background. Using a self-developed simplified backfilling test device, the physical similarity simulation is employed to investigate the seepage behavior of backfill slurry in waste rock aggregates. The effects of slurry concentration, cement–tailing ratio, height of the granular pile, particle size of the granular rock on seepage behavior are analyzed to determine the backfill slurry

concentration that meets on-site fluidity and permeability requirements. Furthermore, by fabricating granular-cemented backfill specimens, the self-supporting capacity and strength variation characteristics of granular-cemented backfill are examined under different slurry concentrations, cement–tailing ratios, and curing ages, with the aim of fulfilling the on-site strength requirements for waste rock-cemented backfilling. The research findings can provide valuable references for similar backfilling projects in other mines.

2. Engineering Background

Shirengou Iron Mine, an Anshan-type magnetite deposit, is situated in Tangshan City, Hebei Province, China. The scope of mining rights in the mine covers the area above the −210 m level, where multiple mining methods have been implemented during production. As shown in Figure 1, the sublevel open stoping with subsequent filling method is adopted for the orebody below the −60 m level. During the mining of the M2 orebody in the −210 m middle section via the filling method, an illegal goaf in the lower section suddenly caves to the stope floor at the −210 m level. Subsequently, the caving height and width of the goaf continued to expand, rapidly extending to the −165 m level with extremely intense caving activity. The resulting goaf is hereinafter referred to as the caving goaf. The illegal goafs refer to underground voids formed by unauthorized civilian mining activities, such as small-scale, unlicensed, or non-compliant mining operations.

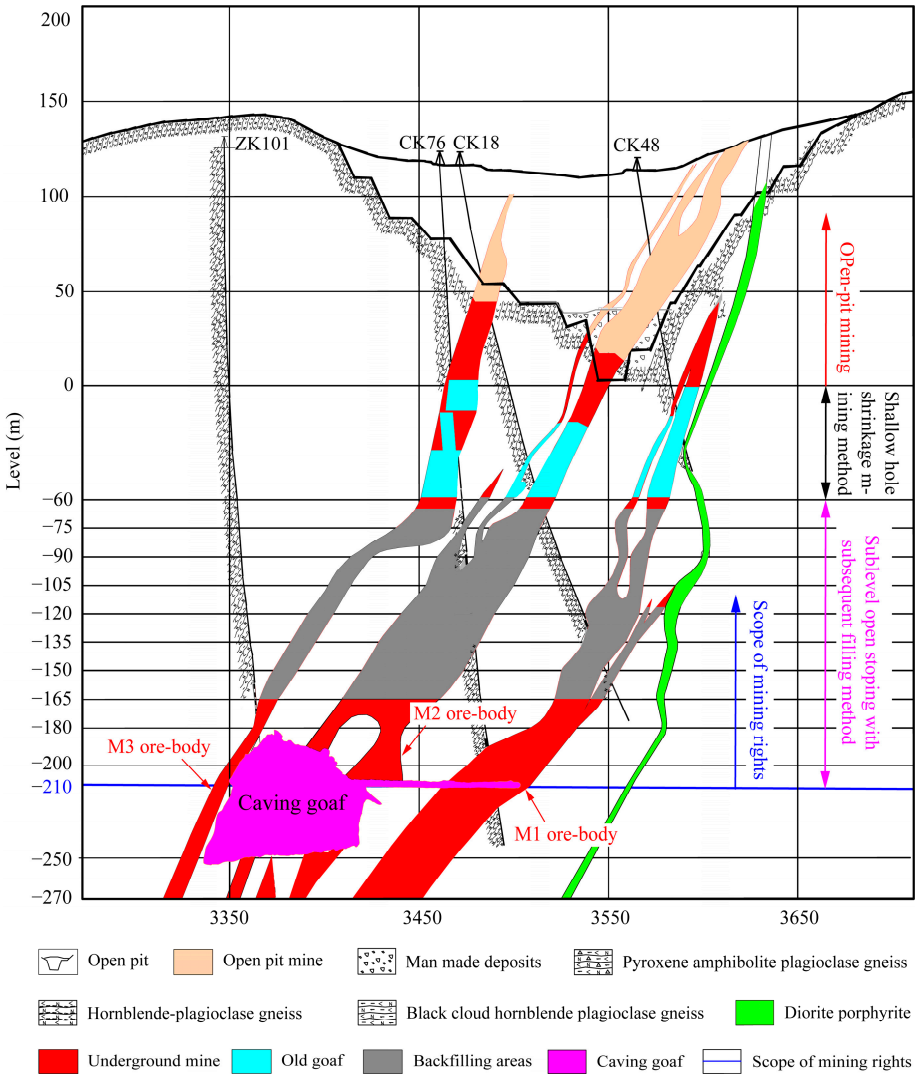


Figure 1. Profile of 10# exploration line in the Shirengou Iron Mine [4]. The scale bar is 1:1000.

The caving goaf is a conservatively estimated volume exceeding 200,000 m^3. The detection results (Figure 2) of the caving goaf are obtained using the FARO Focus S350 3D laser scanner (FARO Technologies, Inc., Lake Mary, FL, USA). Characterized by substantial height, width, and irregularity, the caving goaf features a wider upper section and a narrower lower section with numerous local undulations. As shown in Figure 2, the caving goaf has a height of approximately 120 m, a maximum width of about 102 m along the orebody strike, and a maximum width of roughly 98 m perpendicular to the orebody strike. Above the −240 m level, the roof of the caving goaf approximates a parabolic arch shape. However, below the −240 m level, the goaf floor is inclined and extends overall along the strike direction.

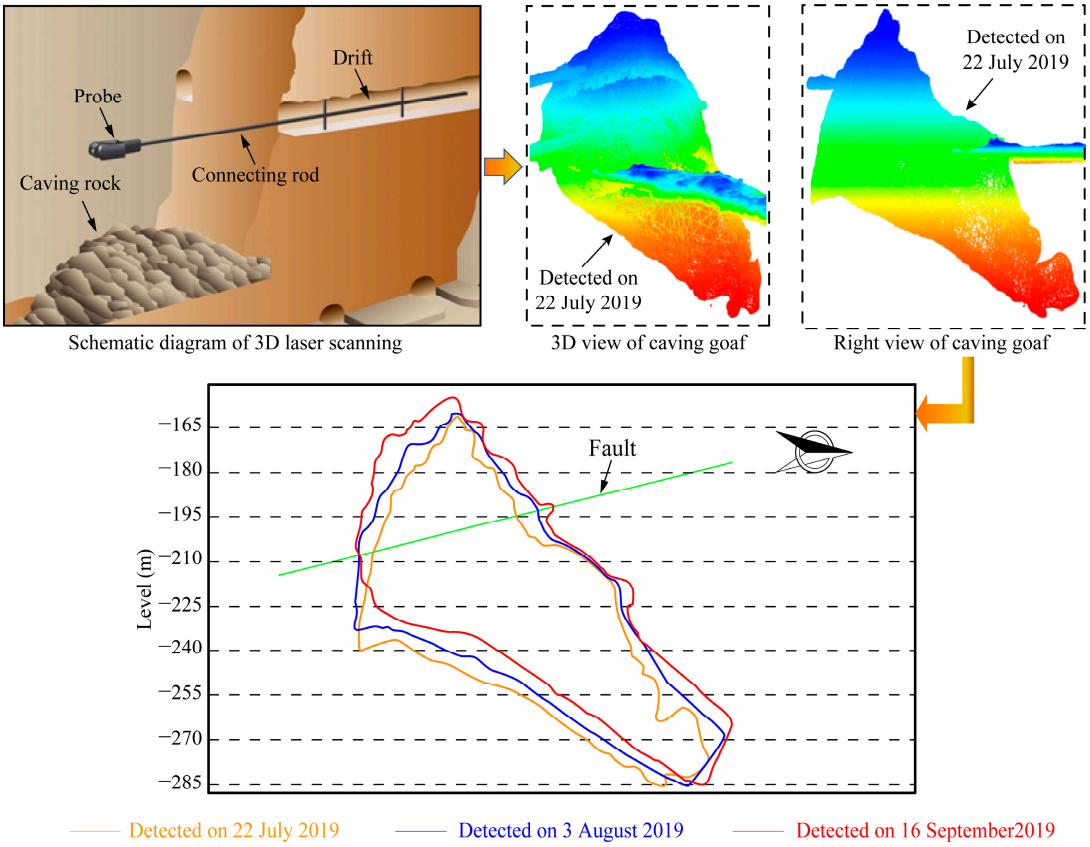


Figure 2. Three-dimensional laser scanning results of the caving goaf. The scale bar is 1:1000.

With a burial depth exceeding 300 m, the safest and most reliable treatment technology for the caving goaf is the filling method. However, during the initial formation stage, the caving goaf undergoes intermittent large-scale collapses over an extended period, resulting in a "simultaneous filling and caving" phenomenon at the filling site. Therefore, when applying the filling method to manage this caving goaf, the experimental for the cemented filling of granular pile must be conducted to ensure the rationality of goaf treatment and the safety of mining in the surrounding orebody.

3. Similarity Design

3.1. Experimental Model

In the design process of the model, the length scale λ_l is usually determined first based on the corresponding conditions of the model's action and the actual test environment, and then the geometric size of the prototype is enlarged (or reduced) by the selected λ_l to obtain the geometric size and boundary conditions of the model. Due to the extremely irregular shape of the caving goaf, to meet the requirements of the indoor experiments, the size of the

bottom of plate of the filling granular rock container is reduced based on the size of the mine floor (40 m thick and 15 m wide), and the length ratio λ_l is 100, the designed filling slurry seepage characteristic experimental device is as shown in Figure 3, when the container size of single-layer filling granular rock in the simple device is 40 cm × 15 cm × 10 cm (length × width × height), the height of the target granular layer is achieved by continuous stacking and the whole process of slurry seepage in the granular layer is recorded by a DV machine.

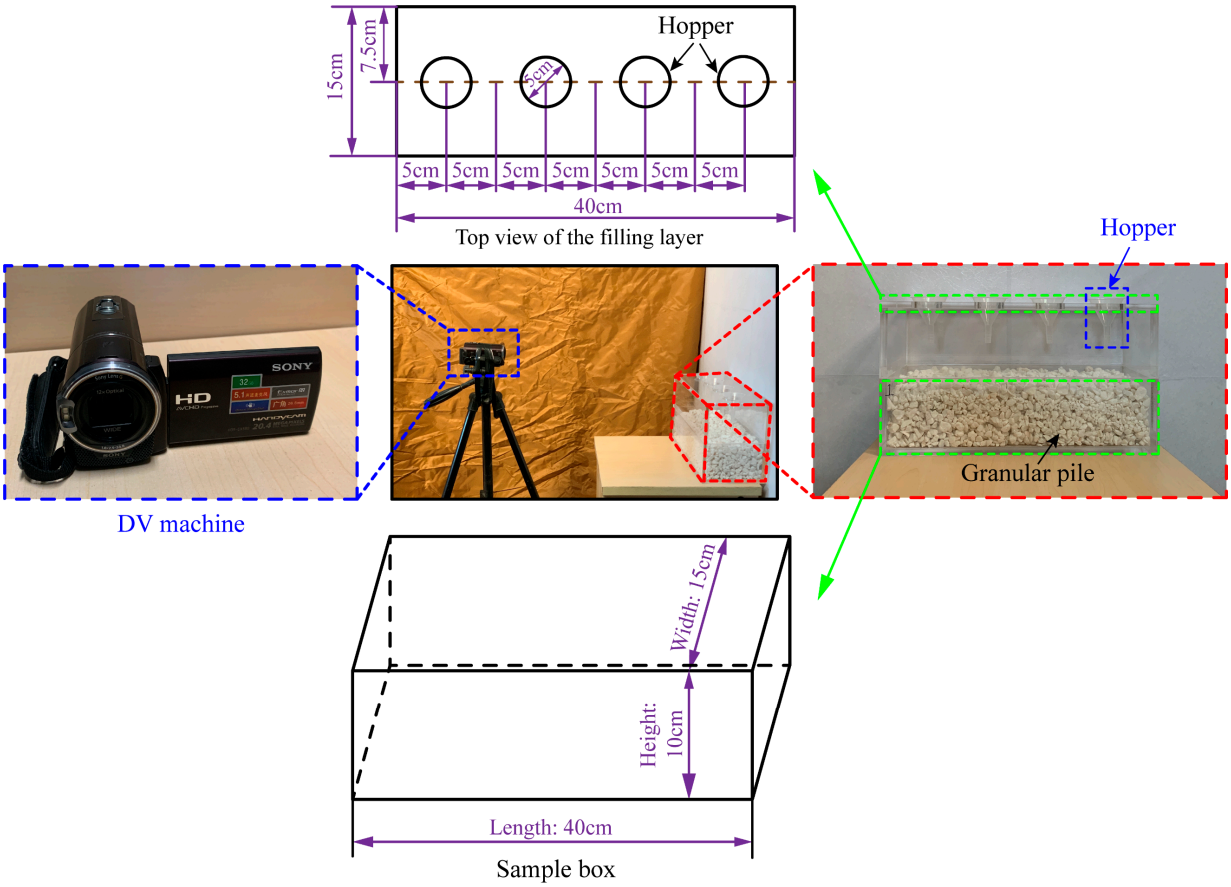


Figure 3. Device of the filling slurry seepage characteristics test.

3.2. Granular Rock

From Figure 2, the goaf caving rock block are accumulated in the bottom plate, increasing the thickness of the bottom plate in the empty area. Thus, the sizes of the accumulated caved rock blocks on the goaf floor can be obtained by the means of 3D laser scanning technology. The particle shape and surface roughness are determined based on the scanning results. Referring to the methodology of laboratory simulation for the random medium ore drawing theory, the equivalent diameter of particles is sufficient to serve as the evaluation index.

Because the level of −225 m~−240 m is close to the level of −210 m, the rock blocks accumulated on the caving goaf can be obtained by encrypted point cloud to configure the experimental similar granular rock. The representative granular heap at the bottom of the caving goaf is selected as shown in Figure 4, and the percentage of the total area of each stage rock block is calculated according to the 28 m × 14 m square grid, so as to estimate the block dimensions of the caving rock, and the calculation equation is

$$\theta_m = \frac{S_m}{S_n} \times 100\% \quad (1)$$

where θ_m is the area percentage of a certain level of rock mass, S_m is the total area of a certain level of rock mass, and S_n is the total area within the measured range.

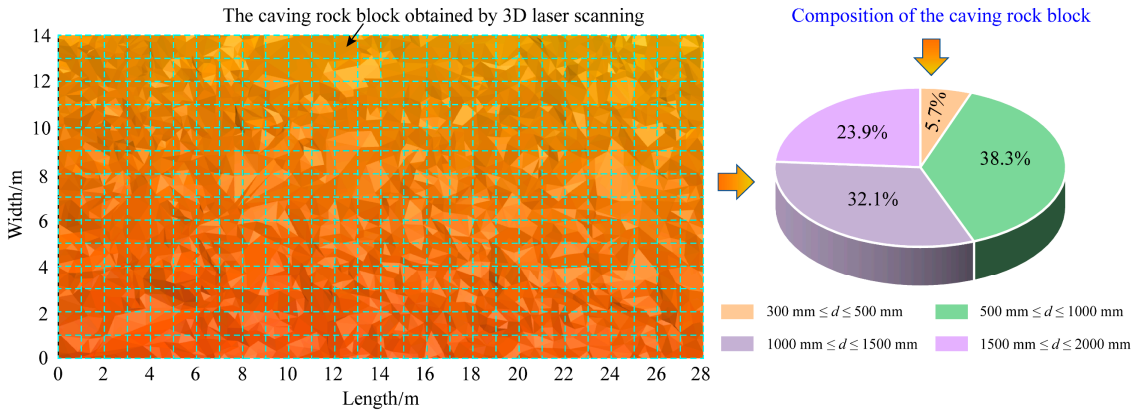


Figure 4. 3D scanning results of goaf caving rock block: the parameter d is the equivalent diameter of the caved rock.

As shown in Figure 4, the block dimensions of the caved rock are estimated according to Equation (1). Considering that the dolomite is commonly used as granular rock [33,34] in the mine release experiment, and its color is also helpful to observe the seepage trajectory and the filling slurry speed, the various sizes of dolomite are selected to the similar granular according to the similar ratio of 1:100. The similar materials of dolomite with different gradation are shown in Figure 5. The dolomite particle size r_g in Figure 5 corresponds to the equivalent diameter of the caved rock d in Figure 4. When simulating the equivalent diameter distribution of caved rock blocks, the gradation ratio of dolomite is as follows: particles with 3 mm < d < 5 mm account for 5.7%, 5 mm < d < 10 mm for 38.3%, 10 mm < d < 15 mm for 32.1%, and 15 mm < d < 20 mm for 23.9%.



(a) 3mm < r_g ≤ 5mm (b) 5mm < r_g ≤ 10mm (c) 10mm < r_g ≤ 15mm (d) 15mm < r_g ≤ 20mm

Figure 5. Test materials of dolomite with different gradation: r_g is the particle size of dolomite, which is one percent of d.

3.3. Filling Slurry

Generally, the fluid employed in the experiment is identical to that acting on the prototype, and fluid experiments should comply with the fluid similarity criteria as closely as possible. However, for seepage experiments of filling slurry within granular piles, satisfying the fluid similarity criteria demands extremely stringent experimental conditions, making it difficult to achieve fluid similarity. This can be explained by the Reynolds criterion in fluid mechanics.

The fluid similarity criteria include the Reynolds criterion, Froude criterion, and Euler criterion. For incompressible steady fluids, dynamic similarity can generally be achieved by satisfying any one of these three criteria. When viscous force is the dominant acting

force, the Reynolds criterion is typically adopted to achieve dynamic similarity, which can be expressed in terms of geometric scale and kinematic scale as follows:

$$\frac{\lambda_l \lambda_v \lambda_\rho}{\lambda_\mu} = 1 \quad (2)$$

where λ_l, λ_v, λ_ρ, and λ_μ are the length scale, velocity scale, fluid density scale, and viscous force scale, respectively. All these scales are determined by the ratio of the corresponding physical quantities of the prototype to those of the model.

When the filling slurry used in the model is the same as that employed in the prototype, both the slurry density scale λ_ρ and the viscous force scale λ_μ are equal to 1. As indicated previously, the length scale λ_l is 100. According to the Reynolds criterion, the velocity scale λ_v is 0.01. In the seepage experiment of filling slurry within granular piles, during the similarity analysis of seepage velocity, the seepage velocity required for experimental similarity cannot be determined because the on-site conditions do not allow for the measurement of seepage velocity within the granular media in caving goaf. However, given that λ_v = 0.01, the seepage velocity of the experimental model should theoretically be 100 times that of the on-site seepage velocity. Conversely, the similarity ratio of the experimental granular media dictates that the size of seepage channels in the experimental granular media is inevitably smaller than that in the on-site granular media. Under the condition that the same filling slurry is used for both the model and the field, the seepage velocity in the experiment will not exceed that in the field. Therefore, to ensure the fluid similarity of this experiment, the filling slurry used in the experiment should be different from that employed in the field.

When the filling slurry used in the model differs from that employed in the field, the research focus shifts to altering the slurry properties, such as density and viscosity coefficient. At a length scale λ_l of 100, the labor intensity of the filling experiment is already substantial. Assuming that the length scale λ_l remains 100 under this scenario; meanwhile, it is difficult to achieve a higher seepage velocity of the slurry in the experiment than that in the field under existing experimental conditions, leading to the condition that $\lambda_v > 1$. According to Equation (2), this further implies that $\lambda_\mu > 100\ \lambda_\rho$. Generally, the filling slurry density does not undergo significant changes; consequently, the corresponding viscosity coefficient would need to exhibit a substantial variation, which is also difficult to achieve under experimental conditions.

Based on the above comprehensive analysis, the filling slurry selected for laboratory tests is consistent with that employed in the field. Considering that the particle size of granular materials and filling rate in the laboratory are far lower than the actual field conditions, the filling slurry mix ratio obtained from laboratory studies can be applied to on-site operations, provided that the laboratory slurry concentration meets the seepage requirements of similar granular piles, and the associated costs and safety criteria are acceptable to the mine.

4. Determination of Material Properties

4.1. Particle Size of Full Tailings

As shown in Table 1, the dimensions of particle size for the full tailings from the Shirengou Iron Mine are measured by the dry sieving method. The particle size of the full tailings ranges from <0.045 mm to 0.5 mm, with the highest content of particles ranging from 0.106 mm to 0.150 mm, and relatively low content of particles above 0.3 mm and below 0.075 mm. The overall distribution shows a normal pattern with small ends and a large middle, and the particle size is relatively small.

Table 1. Dimensions of particle size for the full tailings.

Particle size (mm)	<0.045	0.045~0.075	0.075~0.106	0.106~0.150	0.150~0.30	0.30~0.50
Ratio (%)	2.78	5.25	12.03	49.40	27.47	3.07
Cumulation (%)	2.78	8.03	20.06	69.46	96.93	100

The tailings are composed of particles of different sizes. It can be used to represent the uniformity of the granular level of the material. The larger the uniform coefficient, the more uneven the dimensions of the granular. For the finer particles such as tailings, the following formula can be used to characterize the uniformity of the particles:

$$a = \frac{d_{90}}{d_{10}} \tag{3}$$

where d_{10} and d_{90} are the sieve diameters through which particles with a cumulative content of 10% and 90% can pass, respectively.

As shown in Figure 6, draw the particle size distribution curve of the accumulated tailings passing through the sieve hole diameter based on Table 1. The parameter d_{10} = 81 μm and d_{90} = 264 μm; then, the unevenness coefficient of tailings a = 3.26, indicating that the compactness of the tailings from Shirengou Iron Mine is better.

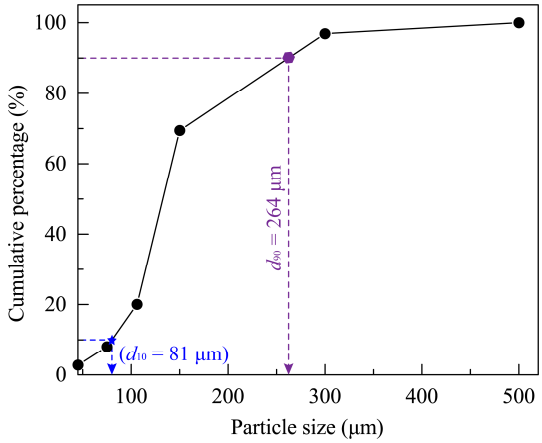


Figure 6. Total tailings particle size distribution curve of Shirengou Iron Mine.

4.2. Collapse Degree of Filling Slurry

The current situation of the caving goaf of Shirengou iron mine is the characteristics of "filling while falling". The flowability of filling slurry in the caving granular rock is one of the main targets for the cemented filling experimental of granular rock. The determination of collapse degree is mainly to master the flowability of filling slurry and determine the slurry concentration C_S with certain fluidity, providing the reference for the maximum slurry concentration in the filling slurry seepage experiment.

Taking the slump experiment with a cement–tailing ratio of 1:4 as an example, the results of the slump are shown in Figure 7. As the concentration of the slurry continues to decrease, the slump of filling slurry continues to increase. The results show that when the slurry concentration is 82%, the material is still scattered or has dry hardness and non-flowability. When the concentration is reduced to 80%, the filling slurry is in a clay-like state with a slump of 43 mm, making it impossible to flow. At a concentration of 78%, the slump of the slurry is 108 mm. Although the slump increases, the slurry is still mostly in a clay-like state and cannot flow within the granular material. When the slurry concentration is reduced to 76%, the slump is 183 mm, and the slurry begins to show fluidity, but it is still not suitable for flowing within the bulk material. When the concentration is 74% to 72%,

the slump is 252 mm to 265 mm, and the fluidity of the slurry is significantly improved. When the concentration is 72%, the slurry is in a relatively thin fluid state. When the slump cone is lifted, the slurry spreads out completely and has a certain degree of flowability.



Figure 7. Slump results of filling slurry: the parameters Cs and T are the slurry concentration and slump, respectively.

Through the slump experiment, it is finally measured that the slurry concentration C_S for the filling slurry with a cement–tailing ratio of 1:4, which exhibits a certain degree of fluidity, is 72%. This value can be adopted as the maximum value of the slurry concentration in the seepage experiment of the filling slurry. As a result, the number of groups in the seepage experiment of the filling slurry is significantly reduced. The slurry concentrations corresponding to other cement–tailing ratios may vary slightly due to differences in tailings content. However, when the concentration reaches 72%, all of them demonstrate a certain level of flowability. Therefore, the slurry concentration is also set at 72% in the seepage experiments of the filling slurry corresponding to other cement–tailing ratios.

4.3. Porosity of Granular Pile

The degree of difficulty of the filling slurry's seepage within the granular pile is related to the porosity of the granular material. Prior to the experiment, it is advisable to first measure the porosity of the granular pile. This can help in understanding the size of the internal voids within different granular piles. The porosity of granular piles is defined as the percentage of the void volume between particles in the total volume of the granular material's accumulation. It is a crucial indicator of the seepage performance of the granular pile and is directly associated with the permeability of the filling slurry and the strength of the granular-cemented backfill. The porosity of the granular piles used in the experiment can be estimated through the drainage method. By utilizing the specimen box depicted in Figure 8 (each specimen box consists of three cube-shaped small specimen boxes with dimensions of 10 cm × 10 cm × 10 cm), the porosity for different particle sizes is measured three times, and then the average value is calculated. The measurement results are presented in Table 2.

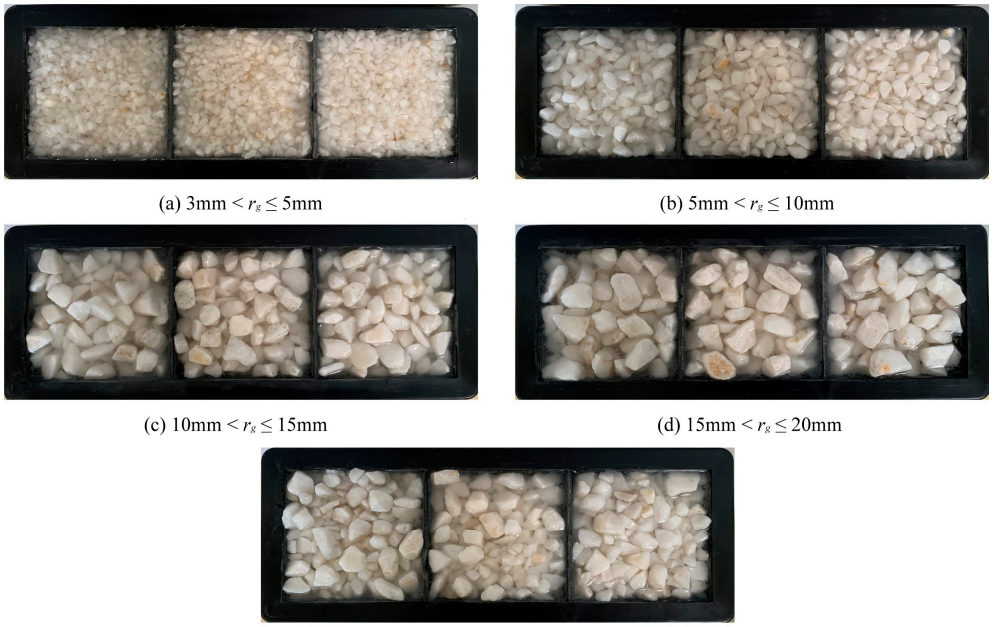


Figure 8. Determination of porosity of granular piles with different sizes: the mixing ratio is a similar dimension of caving rock blocks in the caving goaf.

Table 2. Measurement results of porosity for granular piles.

Granular Particle Size (mm)	Porosity (%)			
	First Time	Second Time	Third Time	Average Value
3–5	40.45	40.75	40.90	40.70
5–10	43.35	43.85	43.65	43.61
10–15	44.55	44.75	45.15	44.82
15–20	45.60	45.85	46.30	45.91
Mixing ratio	44.65	44.70	44.90	44.75

5. Filling Slurry Seepage Law

5.1. Analysis of Influencing Factors

The cemented filling slurry is a mixture of cement, full tailings, and water. The main factors considered in the experiment on its seepage characteristics include slurry concentration C_S, cement–tailing ratio C/T, the height of the granular pile H_g, and the particle size of the granular rock r_g. The cement type employed is slag Portland cement, and the tailings are sourced from the mine's tailings pond.

(1) Slurry concentration C_S

As derived from the slump test of cemented backfill slurry, the concentration corresponding to desirable fluidity is determined to be 72%. Thus, 72% is set as the maximum concentration for the seepage experiment, with test concentrations selected sequentially in descending order to systematically observe and analyze slurry seepage characteristics and granular pile filling performance under different concentrations. Based on the particle size dimensions in Figures 4 and 5, the dosage of single-layer caving granular rock simulator (40 cm × 15 cm × 10 cm) is calculated. As shown in Figure 9, the granular materials are mixed in a container and filled into the experimental device. Subsequently, the filling slurry with different concentrations are individually injected into the granular pile configured according to the mixing ratio.

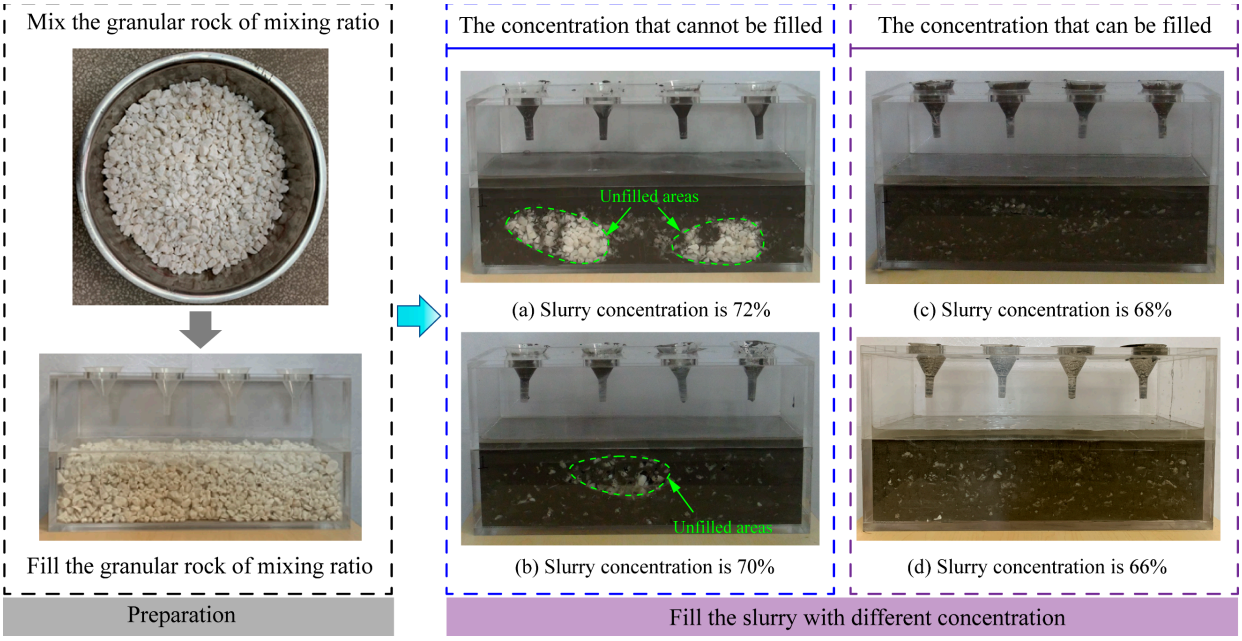


Figure 9. Filling results of different slurry concentration when the cement–tailing ratio is 1:4.

The cemented filling slurry is continuously injected into the granular pile, and the filling process is terminated when the slurry ceased to flow and accumulated persistently on the upper surface of the granular layer. When the cement–tailing ratio (*C*/*T*) is set to 1:4, the filling outcomes corresponding to a slurry concentration (C_S) range of 66%–72% are illustrated in Figure 9. At a slurry concentration of 72% (Figure 9a), the high viscosity of the slurry resulted in sluggish seepage within the granular pile. As the slurry migrated through the pores of the granular pile, it tended to adhere to the surface of the granular pile, consequently forming a compacted slurry layer that inhibited the further seepage of the remaining slurry. This phenomenon ultimately led to incomplete filling of the granular pile by the cemented backfill slurry. Figure 9b depicts the filling performance at a slurry concentration of 70%. At a slurry concentration of 68% (Figure 9c), the cemented filling slurry exhibits uniform seepage behavior within the granular pile, which enabled complete filling of the target voids. Similarly, when the slurry concentration is adjusted to 66% (Figure 9d), complete filling of the bulk is also accomplished.

Figure 10 presents the local filling effects corresponding to slurry concentrations of 72% and 68%. At a slurry concentration of 72%, the high concentration leads to poor fluidity within the granular pile. A compacted slurry layer is prone to form near the upper surface of the granular pile, inhibiting the seepage of the remaining slurry and resulting in unfilled regions in the middle of the granular pile. At a slurry concentration of 68%, the mixture of the granular pile cemented backfill reveals that the granular rock is essentially covered by the slurry. This indicates that at this concentration, the slurry covers the granular pile totally, achieving the favorable filling performance. It is evident that the slurry concentration exerts a significant influence on the seepage behavior. When the height of granular pile is 10 cm and the cement–tailing ratio (*C*/*T*) is 1:4, a compacted slurry layer tends to form near the upper surface when the slurry concentration (C_S) > 68%, leading to incomplete filling of the caving granular layer. In contrast, when $C_S \leq 68\%$, the slurry exhibits superior fluidity within the bulk, enabling complete filling of the caving granular layer.

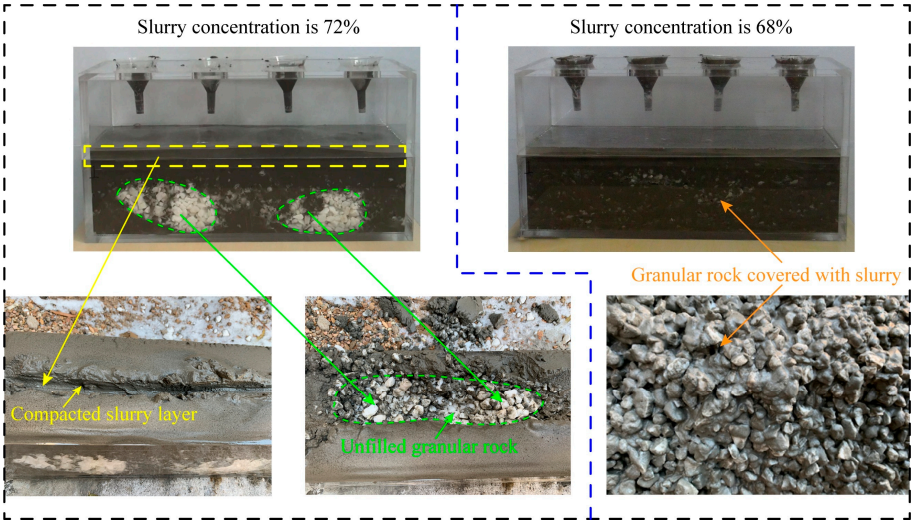


Figure 10. Local filling effect with slurry concentrations of 72% and 68%.

(2) Cement–tailing ratio C/T

From the analysis results of the influence of concentration on slurry seepage, it is found that the filling slurry exhibits favorable fluidity within the granular pile when the slurry concentration is 68%. However, this conclusion is obtained under a fixed cement–tailing ratio (*C/T*) of 1:4, and the seepage behavior of the filling slurry under other *C/T* conditions remains unclear. To investigate the effect of different cement–tailing ratios on slurry seepage, four groups of *C/T* values (1:4, 1:6, 1:8, and 1:12) are selected for the experiment. The experimental parameters are set as follows: slurry concentration of 68%, granular pile height of 10 cm, and granular rock particle sizes are consistent with the mixing ratio. Cemented filling slurry is continuously injected into the granular pile, and the filling process is terminated when the slurry ceased to flow and accumulated persistently on the upper surface of the granular layer. Subsequently, the granular-cemented backfill composite is allowed to stand for 10 min to observe the settlement of the filling slurry within the granular pile.

The filling effects corresponding to different cement–tailing ratio are presented in Figure 11. The filling slurry in all four selected *C/T* groups achieves complete filling of the granular pile, and the slurry seepage trajectory during the filling process and the granular-cemented backfill effect are basically consistent. The filling results in Figure 11 indicate that the cement–tailing ratio has a negligible influence on the seepage of the filling slurry within the granular pile. This phenomenon may be attributed to the fine particle size of the tailings. The cemented filling slurry is a mixture of cement, tailings, and water. At a fixed concentration, the mass of solute contained in the filling slurry is the same for different cement–tailing ratios, but the tailings content varies significantly. If the particle size of tailings is larger, it should inevitably exert a significant impact on the seepage of the filling slurry within the granular pile. As shown in Table 1, the tailings have a fine particle size, so it can be inferred that the cement–tailing ratio has little effect on the seepage of the filling slurry within the granular pile under other concentrations. Nevertheless, it does not rule out the possibility that the cement–tailing ratio may not affect the slurry seepage for other tailings particle size grades.

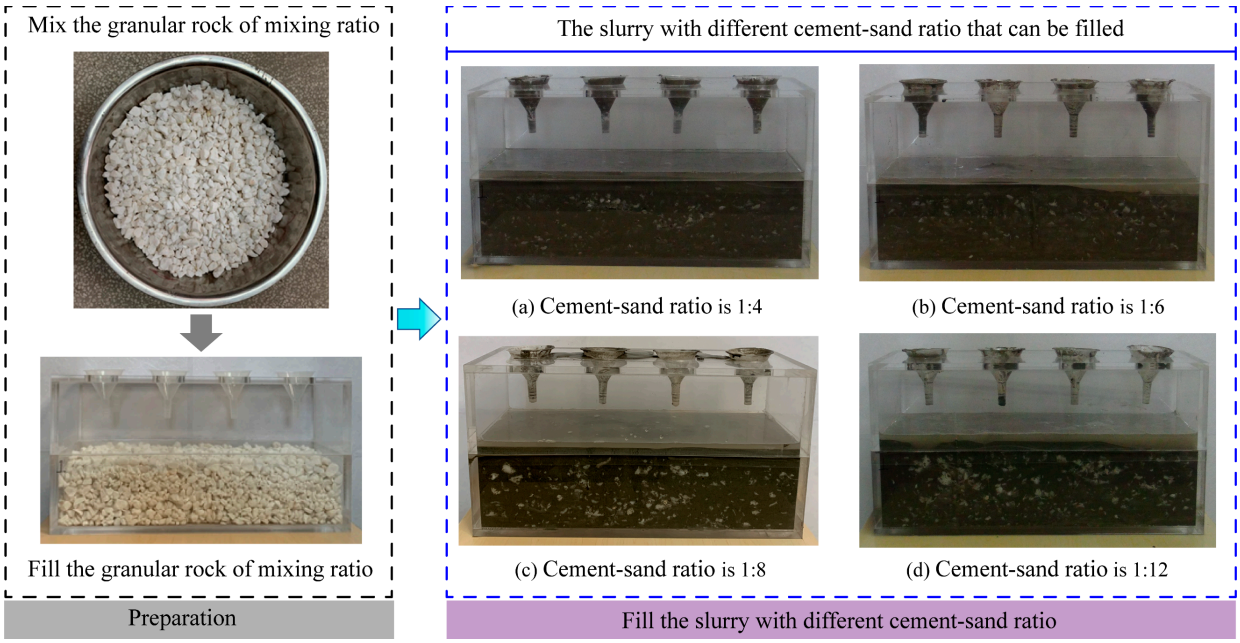


Figure 11. Filling results of different cement–tailing ratio when the slurry concentration is 68%.

(3) Height of the granular pile H_g

When analyzing the effects of slurry concentration and cement–tailing ratio (*C*/*T*) on the seepage behavior of filling slurry, the height of the granular pile (H_g) is consistently fixed at 10 cm. To investigate the influence of pile height on slurry seepage, three test groups with pile heights of 10 cm, 20 cm, and 30 cm are designed. As shown in Figure 12, the container for single-layer granular pile has dimensions of 40 cm × 15 cm × 10 cm (length × width × height), and the target pile height is achieved through sequential stacking. The experimental parameters are standardized as follows: slurry concentration of 68%, cement–tailing ratio (*C*/*T*) of 1:4, and granular rock particle sizes are consistent with the mixing ratio. Cemented filling slurry is continuously injected into the granular pile, and the filling process is terminated when the slurry ceased to flow and accumulated persistently on the upper surface of the granular layer. Subsequently, the granular-cemented backfill composite is allowed to stand for 10 min to observe the settlement of the filling slurry within the granular pile.

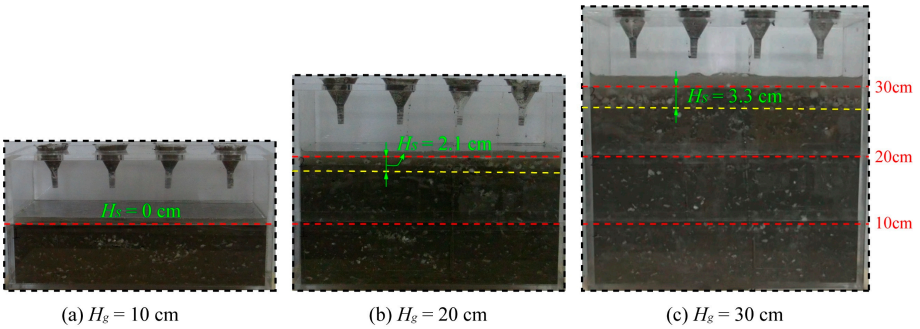


Figure 12. Filling result of different granular pile height: H_s is the slurry settlement height on the surface of the filling layer.

The filling effects corresponding to different pile heights are presented in Figure 12. Under the conditions of a slurry concentration of 68%, a cement–tailing ratio (*C*/*T*) of 1:4, and granular rock particle size consist with the mixing ratio, the filling slurry achieved effective filling for all three selected pile heights. The filling slurry is typically in a fully

saturated state at the initial stage of filling. Upon being injected into the granular pile, the slurry gradually undergoes settlement over time under the combined action of capillary pressure and the self-weight of solid particles. As shown in Figure 12, the settlement of the filling slurry is negligible when the pile height is 10 cm. With the pile height increased to 20 cm, the slurry exhibits significant settlement (H_S = 2.1 cm), and this settlement phenomenon became even more pronounced at a pile height of 30 cm (H_S = 3.3 cm). These results indicate that under the control of constant slurry concentration, cement–tailing ratio, and particle size, the settlement degree of the filling slurry becomes increasingly remarkable with the increase in pile height.

(4) Particle size of the granular rock r_g

When analyzing the effects of slurry concentration, cement–tailing ratio (*C*/*T*), and pile height on the seepage behavior of filling slurry, the granular rock particle size is consistently fixed as the mixing ratio. As shown in Table 2, the porosity of the granular pile is proportional to the particle size, implying that the seepage characteristics of the filling slurry are expected to differ under varying granular particle size conditions. To systematically investigate the influence of particle size on slurry seepage, according to Table 2, four particle size configurations are selected: 3–5 mm, 5–10 mm, 10–15 mm, and the mixing ratio. The experimental parameters are standardized as follows: slurry concentration of 68% and cement–tailing ratio (*C*/*T*) of 1:4. To facilitate better comparison and observation of the effects of different granular particle sizes, the packing container for granular rock is designed with dimensions of 10 cm × 10 cm × 65 cm (length × width × height) and the pile height is set as 60 cm. Cemented filling slurry is continuously injected into the granular pile, and the filling process is terminated when the slurry ceased to flow and accumulated persistently on the upper surface of the granular layer. Subsequently, the granular-cemented backfill composite is allowed to stand for 10 min to observe the settlement of the filling slurry within the granular pile.

Figure 13 presents the comparative results of the granular pile before and after filling for different particle sizes following the 10 min standing period post-filling. When the granular particle size (r_g) ranged from 3 to 5 mm (Figure 13a), the relatively low internal porosity of the granular pile leads to the formation of a compacted slurry layer at the top of the pile during slurry pouring. Consequently, the 68% concentration slurry fails to completely fill the granular pile with 60 cm height, with the maximum achievable filling height limited to approximately 15 cm. For the particle size range of 5–10 mm (Figure 13b), the 68% concentration slurry achieved near-complete filling of the granular pile with 60 cm height. However, the formation of a compacted slurry layer at the top resulted in partially unfilled regions in the middle of the bulk pile. When r_g ranged from 10 to 15 mm (Figure 13c), complete filling of the granular pile with 60 cm height is achieved, consistent with the performance observed for the mixing ratio (Figure 13d). However, the pile porosity under the 10–15 mm particle size condition is higher than that of the mixing ratio (as shown in Table 2), which leads to a significant enhancement in the seepage velocity of the filling slurry within the granular pile. Simultaneously, the settlement height after 10 min of standing is also increased. Collectively, the filling results for different granular particle sizes demonstrate that the smaller the particle size, the more pronounced the resistance to slurry seepage within the granular pile. Furthermore, when the slurry concentration is sufficient to achieve complete granular pile filling, a higher pile porosity corresponds to a greater settlement height at the top of the filled granular pile.

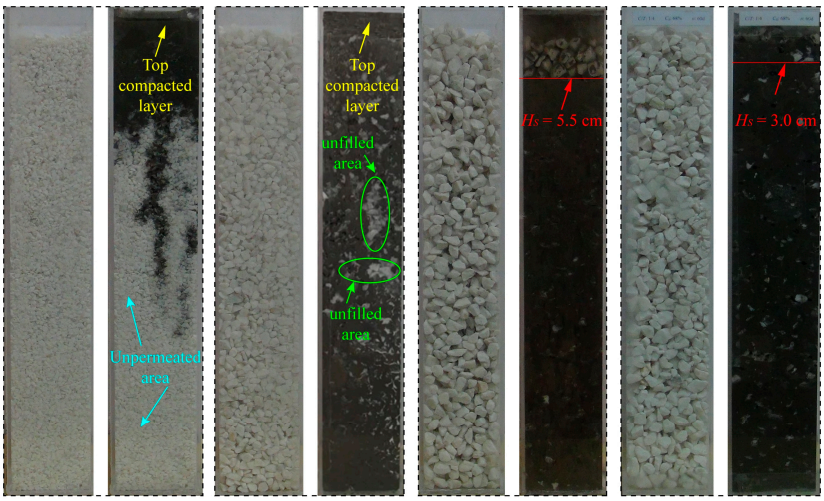


Figure 13. Comparison of granular materials with different particle sizes before and after filling.

5.2. Critical Concentration of Filling Slurry

On-site investigation and analysis reveal a granular pile with a height of approximately 50–60 m in the caving goaf of Shirengou Iron Mine. As previously discussed, the cement–tailing ratio exerts a relatively minor impact on the seepage of filling slurry within the granular layer. Specifically, the height of granular pile primarily affects the settlement of filling slurry inside the granular layer, while the particle size of granular materials mainly influences the seepage height of filling slurry within the granular pile. To determine the optimal concentration of slurry for caving goaf filling, the laboratory similarity experiments are conducted with the following parameters: a cement–tailing ratio of 1:4, a granular pile height of 60 cm, and a particle size consistent with the mixing ratio.

Figure 14 illustrates the filling results corresponding to different slurry concentrations when the granular pile height is 60 cm. Under the conditions of a 1:4 cement–tailing ratio and granular particle sizes consistent with the mixing ratio, filling slurries with concentrations of 70% and 69% formed a compacted top layer during filling. This compacted layer prevents further seepage of the remaining slurry, thus precluding complete filling of the granular layer. In contrast, slurries with concentrations of 68% and 64% achieved full filling of the granular layer. After filling completion and during static placement, tailings continuously settle under the combined action of capillary pressure within the slurry and the self-weight of solid particles. A certain degree of settlement is observed in both slurries after 10 min of static placement, with the settlement height increasing as the slurry concentration decreased.

Based on the analysis of the influencing factors of backfilling seepage and the filling simulation under on-site operating conditions (as shown in Figure 14), it can be concluded that with the further refinement of slurry concentration, the backfill slurry cannot fully fill the granular piles when the slurry concentration is 70% and 69%. Besides the compacted layer at the top, the particle compaction effect resulting from the increase in granular pile height also affects the seepage of backfill slurry. When the slurry concentration is 68% and 64%, the backfill slurry exhibits excellent fluidity within the granular layer, facilitating the sufficient filling of granular piles. Additionally, lower concentrations correspond to greater tailing settlement heights. In accordance with the definition of the critical seepage concentration for filling slurry, the critical concentration is appropriately determined as 68% for the granular pile of caving goaf.

The filling effect of the 68% concentration slurry, captured from a clockwise-rotated perspective, is presented in Figure 15, which shows the filling conditions of the front, right,

back, and left sides. Both the front (Figure 15a) and back (Figure 15c) filling effects indicate that the slurry exhibits more significant settlement in the central area of the top layer than at both ends. In Figure 15a, a local compacted layer formed in the top-right region, resulting in no settlement on the right side (Figure 15b). On the left side, the filling effect (Figure 15d) shows a significantly smaller top-layer settlement height, which is attributed to the seepage of slurry within the granular layer. Based on a physical similarity ratio of 1:100, it can be confirmed that the 68% concentration filling slurry can fully fill the caved rock layer in the goaf and achieve favorable filling effects at both ends, thereby demonstrating applicability to practical engineering scenarios.

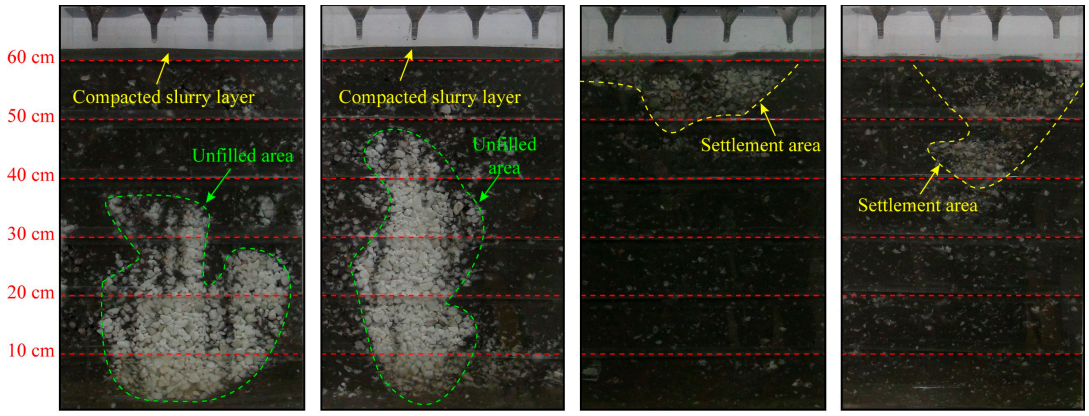


Figure 14. Filling results of different slurry concentration at the 60 cm granular pile height.

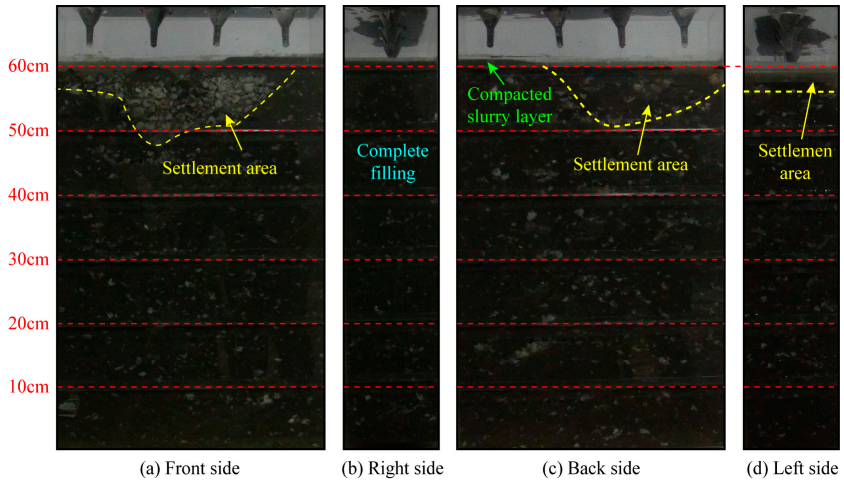


Figure 15. Filling effect with a slurry concentration of 68%.

6. Strength Characteristics for Granular-Cemented Backfill

6.1. Sample Preparation

As previously established, the critical concentration of filling slurry for seepage through the granular pile is 68%, at which the settlement performance is also favorable. To ensure the safety of on-site filling, strength tests for the granular-cemented backfill are designed. The filling slurry is prepared with three cement–tailing ratios (1:4, 1:8, 1:12) and three concentrations (72%, 68%, 64%). Each combination is used to fill the simulated granular pile of caving goaf. The strength tests are conducted at three curing ages (14 d, 28 d, 60 d) after filling.

The internal dimensions of the mold for granular-cemented backfill samples are 10 cm × 10 cm × 65 cm (length × width × height). The mold is fabricated from 3 mm-

thick acrylic sheets, with the granular material packed to a height of 60 cm. The filling slurry is formulated by combining the designed cement–tailing ratio and concentrations, yielding the granular-cemented backfill samples as shown in Figure 16.

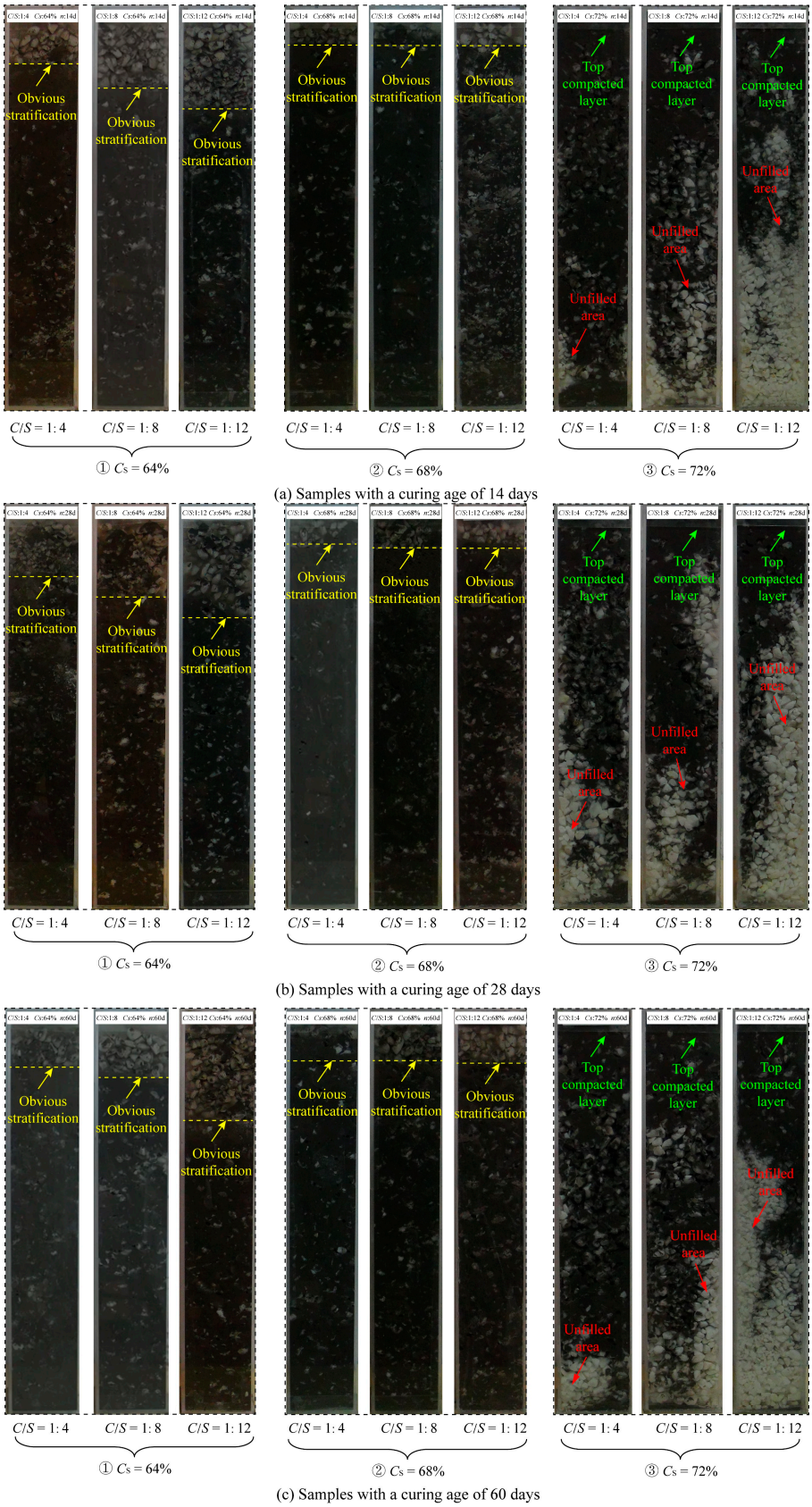


Figure 16. Granular-cemented backfill sample.

The filling results for different slurries in Figure 16 are generally consistent with the seepage characteristic test results. A discrepancy between the filling results in Figure 16 and the seepage test results is observed as follows: when $C_S \leq 68\%$, although the slurry consistently achieves complete filling, the cement–tailing ratio exerts no influence on the seepage behavior inside the granular layer (attributed to the fine particle size of tailings), but significantly affects slurry settlement. At $C_S = 64\%$, smaller cement–tailing ratio leads to more pronounced settlement. At $C_S = 68\%$, variations in cement–tailing ratio have minimal impact on settlement, which is because the high-concentration slurry effectively fills the internal pores of the granular layer, thereby suppressing settlement. Therefore, the preparation of granular-cemented backfill samples not only provides samples for strength testing but also effectively supplements the experimental data on the seepage characteristics of cemented filling slurry.

It is evident that once the granular layer reaches a certain height, the factors affecting filling slurry settlement become complex, involving the cement–tailing ratio, slurry concentration, and granular pile porosity. This study focuses solely on the backfilling treatment of caving goaf in the Shirengou Iron Mine. The intrinsic mechanisms and microscopic mechanisms underlying the influences of relevant factors will be discussed in detail in the subsequent research work.

6.2. Strength Test

After the fabrication of granular-cemented backfill samples, all samples with a slurry concentration $C_S \leq 68\%$ exhibit a certain degree of top settlement. Upon complete settlement, a specific height of standing water remains above the sample boxes, which isolates the sample surfaces from air, prevents water evaporation within the granular-cemented backfill, and thus ensures sufficient hydration of the cementitious materials. However, the bleeding water negatively affects the strength of the final product, which is consistent with the operating conditions of actual underground backfilling sites. Seven days after specimen fabrication, residual standing water above the samples is drained based on the compaction degree of granular particles and backfill materials inside the samples.

As shown in Figure 17, the drainage cut-off line is generally lower than the obvious stratification line observed during the initial filling stage, suggesting that the filling slurry do not achieve the maximum natural settlement initially. Due to the large particle size of the granular materials within the backfill, formwork removal is only conducted after the filling slurry and granular particles have fully set (typically approximately 7 days post-drainage).

Figure 17 further demonstrates that after formwork removal, when $C_S \leq 68\%$, the sum of the self-supporting cemented height of the granular-cemented backfill and the drainage height are equal to the filling height (as shown in Table 3). In contrast, when $C_S > 68\%$, the filling slurry exhibits low permeability. The slurry that permeated to the lower layer is insufficient to cement the granular layer, resulting in a relatively small self-supporting cemented height. Notably, the self-supporting height decreases with a reduction in the cement–tailing ratio. This observation confirms that the better the bonding between the filling slurry and the granular layer (achieved when the slurry fully fills the caved granular layer), the greater the self-supporting cemented height of the granular layer.

After formwork removal, the granular-cemented backfill samples have insufficient strength to meet the test requirements, as they need to be cured in the formwork for an extended period with minimal air contact. These samples require additional curing at room temperature (20–23 °C), with the curing age calculated from the date of formwork removal. The filling height, drainage height, and self-supporting height of each sample are detailed in Table 3.

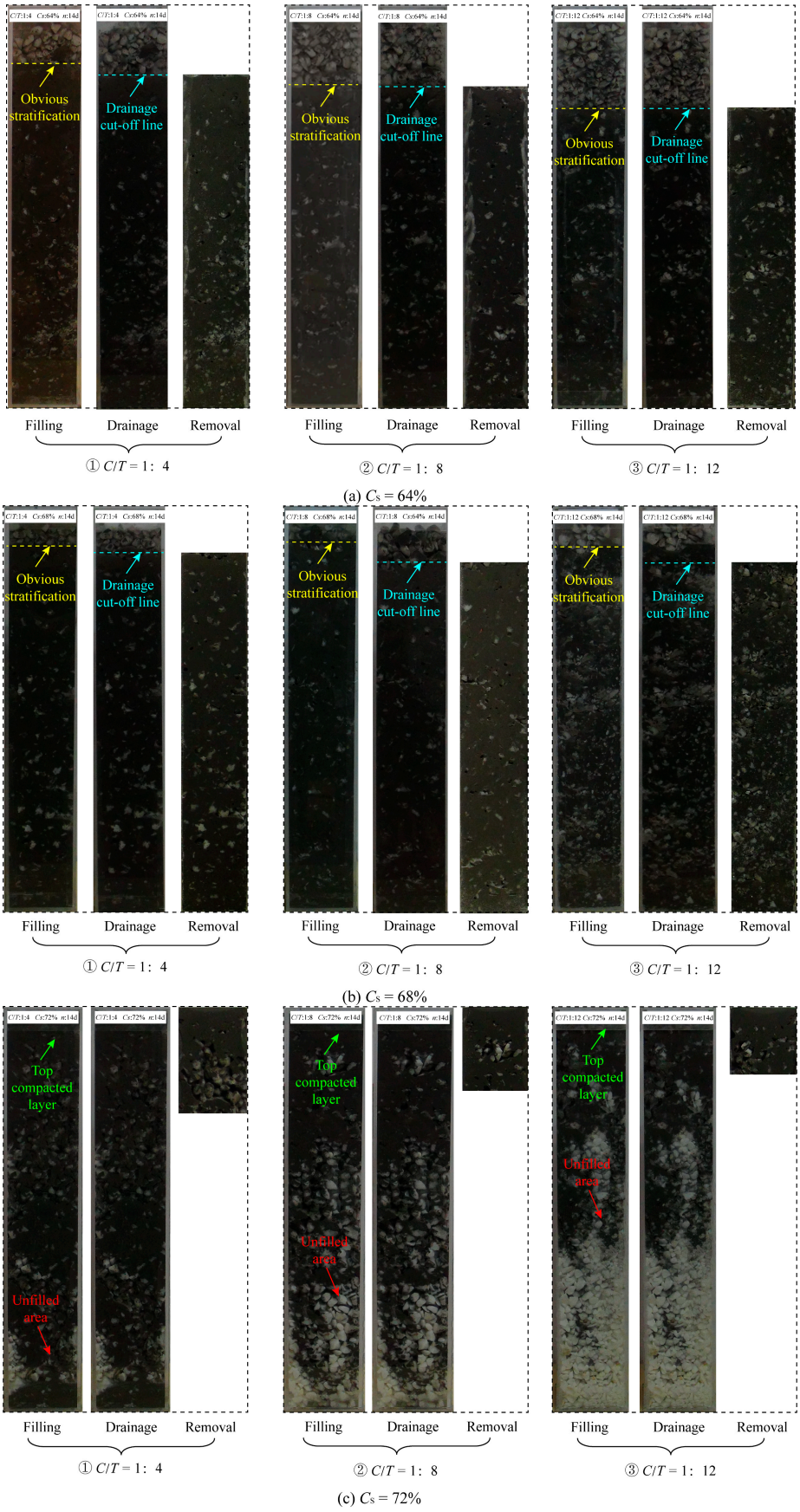


Figure 17. Drainage and removal of samples with curing age of 14 days.

Table 3. Test data of granular-cemented backfill.

Curing Age (d)	Slurry Concentration (%)	Cement–Tailing Ratio	Filling Height (cm)	Drainage Height (cm)	Self-Supporting Height (cm)	Compressive Area (cm^2)	Failure Load (kN)	Compressive Strength (MPa)
14	64%	1:4	60	10.4	49.6	9.6 × 9.6	10.69	0.986
		1:8	60	11.6	48.4	9.6 × 9.8	6.21	0.584
		1:12	60	15.0	45.0	9.5 × 9.6	3.54	0.323
	68%	1:4	60	6.7	53.3	10 × 10	11.43	1.143
		1:8	60	8.3	51.7	10 × 10	7.82	0.782
		1:12	60	8.6	51.4	9.8 × 10	6.06	0.594
	72%	1:4	60	0	15.8	10 × 10	15.82	1.582
		1:8	60	0	13.3	10 × 10	9.45	0.945
		1:12	60	0	10.8	10 × 10	7.57	0.757
28	64%	1:4	60	11.4	48.6	9.8 × 9.8	17.61	1.691
		1:8	60	12.5	47.5	9.7 × 9.7	6.89	0.649
		1:12	60	16.2	43.8	9.5 × 9.7	4.10	0.378
	68%	1:4	60	6.9	53.1	10 × 10	20.71	2.071
		1:8	60	8.5	51.5	10 × 10	9.52	0.952
		1:12	60	9.1	50.9	10 × 10	6.02	0.602
	72%	1:4	60	0	15.6	10 × 10	28.37	2.837
		1:8	60	0	12.5	10 × 10	12.66	1.266
		1:12	60	0	11.2	10 × 10	8.93	0.893
60	64%	1:4	60	10.2	49.8	10 × 10	20.64	2.064
		1:8	60	10.8	49.2	10 × 10	8.35	0.835
		1:12	60	15.3	44.7	9.8 × 9.8	4.28	0.411
	68%	1:4	60	6.5	53.5	10 × 10	29.83	2.983
		1:8	60	8.7	51.3	10 × 10	11.76	1.176
		1:12	60	9.4	50.6	10 × 10	6.83	0.683
	72%	1:4	60	0	15.3	10 × 10	37.12	3.712
		1:8	60	0	14.1	10 × 10	13.92	1.392
		1:12	60	0	12.8	10 × 10	9.25	0.925

Following formwork removal, the samples are cured for 14, 28, and 60 days respectively, and their uniaxial compressive strength is measured using a compression–shear testing machine. Taking the 14-day cured samples as an example, the dimensions of the granular-cemented backfill samples vary with slurry concentration (Figure 18a). Prior to strength testing, these samples required cutting (Figure 18b) into standard specimens. During sample cutting, it is essential to ensure that the sample remains horizontal and that an adequate buffer layer is placed underneath it. The operation should follow the protocol of one person performing the cutting and another monitoring the process. Since the cutting duration is relatively short, this process exerts a minimal influence on both the internal damage to the sample and its mechanical strength.

Due to the influence of slurry seepage, the rock strength at the top of the sample is the minimum. To meet the field filling requirements, it is necessary to ensure that the top of the sample meets the strength requirements as much as possible. Therefore, to ensure comparability of strength results, cutting is primarily performed near the top of the samples, with the cut dimensions adjusted to approximate a 10 cm cube as closely as possible. The standard specimens are then placed in a rigid rock testing machine (Figure 18c) to determine their uniaxial compressive strength. The compressive area, failure load, and compressive strength of each specimen are summarized in Table 3.

Figure 19 shows the bar charts and exponential nonlinear fitting curves of the cement–tailing ratio versus sample strength corresponding to three curing ages. The results indicate that the effect of the cement–tailing ratio on strength follows an obvious exponential law, demonstrating that a higher slurry concentration exerts a more intense influence on backfill strength. Furthermore, an increased cement–tailing ratio gives rise to a more

dramatic exponential growth, which implies that a faster increase in the cement–tailing ratio corresponds to a higher sample strength.

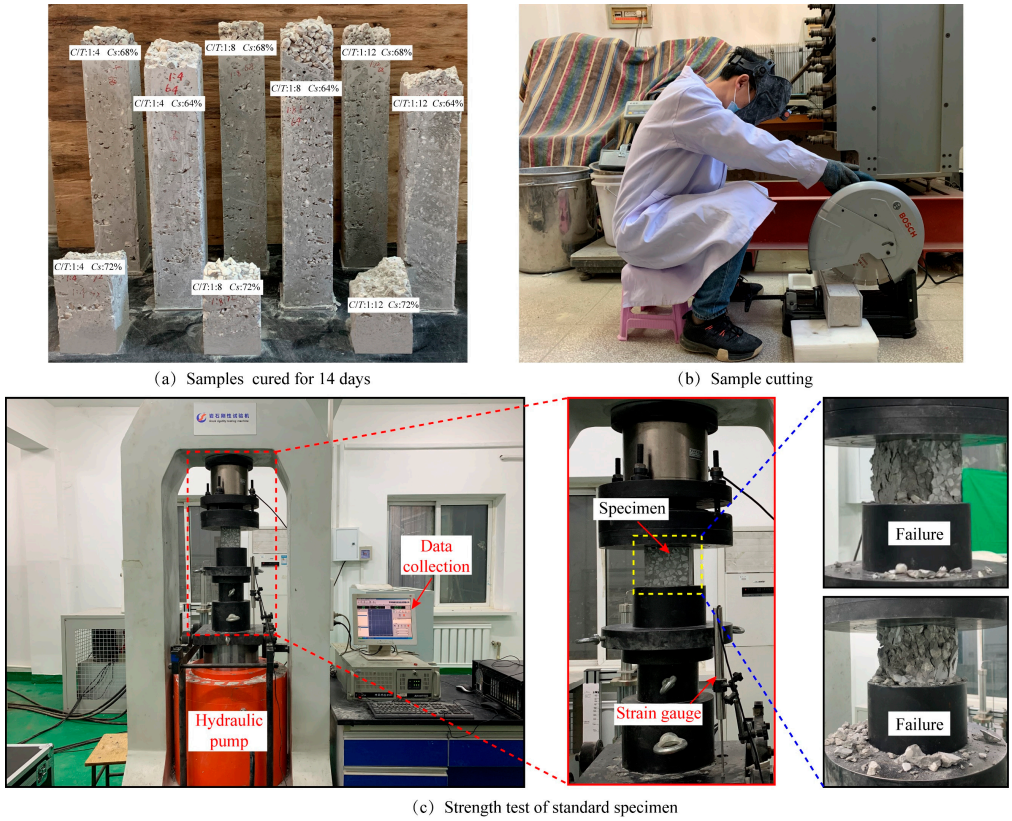
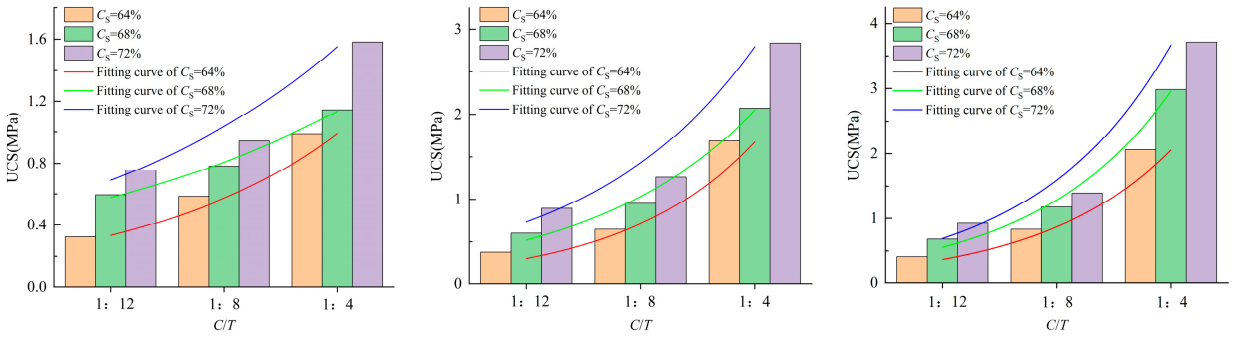


Figure 18. Determination of uniaxial compressive strength of specimens.



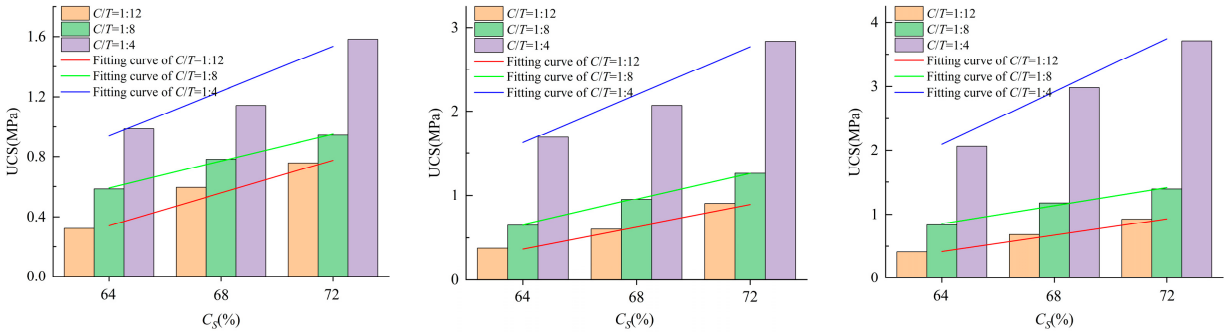
(**a**) n = 14d (**b**) n = 28d (**c**) n = 60d

Figure 19. Exponential fitting curve of cement–tailing ratio and backfill strength: where *Cs* is slurry concentration, C/T is the cement–tailing ratio, and n is curing age.

Figure 20 depicts the bar charts and linear fitting curves of slurry concentration versus sample strength corresponding to three curing ages. The results show that the effect of slurry concentration on backfill strength exhibits an obvious linear regularity, indicating that under the condition of the same cement–tailing ratio, the strength of backfill increases linearly with the rise in slurry concentration when the effect of seepage flow is not considered.

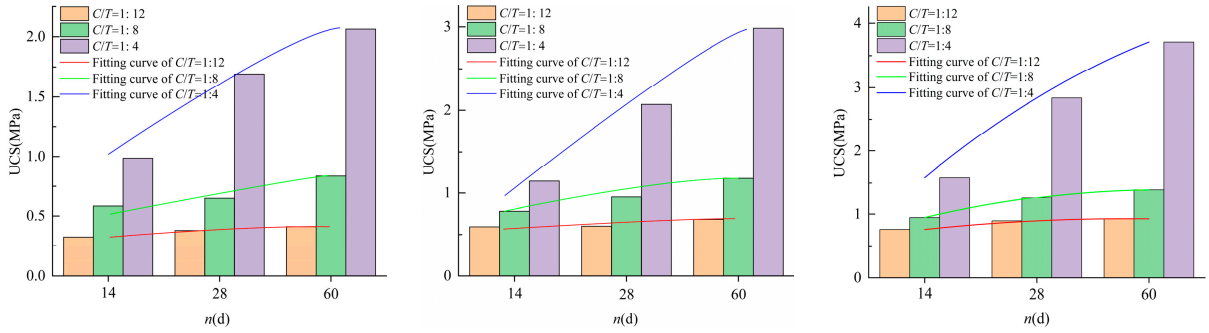
Figure 21 shows the bar charts and power function nonlinear fitting curves of curing age versus sample strength corresponding to three slurry concentrations. The results indicate that the effect of curing age on UCS strength follows an obvious power function

law, demonstrating that in the initial stage, the strength growth rate is relatively fast, and after a certain period of time, the strength growth rate tends to slow down.



(**a**) n = 14d (**b**) n = 28d (**c**) n = 60d

Figure 20. Linear fitting curve of slurry concentration and backfill strength: where *Cs* is slurry concentration, C/T is the cement–tailing ratio, and n is curing age.



(**a**) Cs = 64% (**b**) Cs = 68% (**c**) Cs = 72%

Figure 21. Power function fitting curve of curing age and backfill strength: where *Cs* is slurry concentration, C/T is the cement–tailing ratio, and n is curing age.

6.3. Sensitivity Analysis

In the cemented filling experiment of caving granular rock, the strength of the filling body is mainly correlated with slurry concentration, cement–tailing ratio, and curing age. An orthogonal test is conducted to clarify the sensitivity of these three factors to the filling body strength. Specifically, three levels are set for each factor: cement–tailing ratios of 1:4, 1:8, and 1:12; slurry concentrations of 64%, 68%, and 72%; and curing ages of 14 d, 28 d, and 60 d. Based on this design, the sensitivity of each factor to the filling body strength is investigated.

In the orthogonal test, distinct influencing factors are denoted as A, B, C, ..., and the parameter q represents the number of levels for each factor. Let A_m denote the m-th level value of factor A (m = 1, 2, 3, ..., q), and X_m denote the m-th level value of factor n (m = 1, 2, 3, ..., q; n = A, B, ...). Orthogonal tests are designed under the condition of X_m, yielding the evaluation index value Y_{mn} corresponding to the m-th level of factor n. Y_{mn} is a random variable following a normal distribution. When n orthogonal tests are performed under X_m, w results are obtained, denoted as Y_{mnk} (k = 1, 2, 3, ..., w), leading to the following equation:

$$K_{mn} = \frac{1}{w}\sum_{k=1}^{w} Y_{mnk} \quad (4)$$

where the parameter K_{mn} is the statistical parameter of the influencing factor n at the m-th level value.

The sensitivity of each influencing factor is evaluated by the magnitude of the range R_n. The calculation equation is as follows:

$$R_n = \max\{K_{1n}, K_{2n}, \ldots, K_{qn}\} - \min\{K_{1n}, K_{2n}, \ldots, K_{qn}\} \quad (5)$$

A larger range R_n indicates a more significant impact of the influencing factor's level variation on the evaluation index. Thus, the sensitivity of each influencing factor to the evaluation index can be analyzed by ranking the range values.

In analysis of variance (ANOVA) calculations, the significance is determined by comparing the calculated *F*-value with the tabulated *F*-value. The latter is obtained from statistical tables based on three variables: the selected confidence level (i.e., significance level), factor degrees of freedom, and error degrees of freedom. If the calculated *F*-value exceeds the tabulated *F*-value, the factor exerts a significant effect on the target variable at the specified significance level.

Based on the filling material proportioning tests and the on-site working conditions of Shirengou Iron Mine, the uniaxial compressive strength (UCS) of the granular-cemented backfill is selected as the evaluation index for this orthogonal analysis. The key influencing factors include cement–tailing ratio, slurry concentration, and curing age, with their corresponding levels listed in Table 4.

Table 4. Orthogonal test factor level.

Level	Factor Value		
	A **(Cement–Tailing Ratio)**	***B*** **(Slurry Concentrations)**	***C*** **(Curing Age)**
1	1:4	64%	14 d
2	1:8	68%	28 d
3	1:12	72%	60 d

This study adopts a three-factor, three-level orthogonal test design, where interactions between factors are considered. The orthogonal array $L_9(3^4)$ is employed for test arrangement. For computational convenience, the cement–tailing ratio and slurry concentration are converted into numerical values: cement–tailing ratios of 1:4, 1:8, and 1:12 are converted to 0.25, 0.125, and 0.083, respectively; slurry concentrations of 64%, 68%, and 72% are converted to 0.64, 0.68, and 0.72, respectively. The orthogonal test design, established using SPSS V26.0.0 software, is presented in Table 5.

Table 5. Orthogonal test results.

Group Number	Factor			Indicator
	A	***B***	***C***	
1	1	1	1	0.986
2	1	2	2	2.071
3	1	3	3	3.712
4	2	1	3	0.835
5	2	2	1	0.782
6	2	3	2	1.266
7	3	1	2	0.378
8	3	2	3	0.683
9	3	3	1	0.757

Range analysis and ANOVA are performed on the orthogonal test data via SPSS to quantify the sensitivity of the three factors to the UCS of the granular-cemented backfill.

The range analysis results are shown in Table 6, which indicates that the factors ranked by range value (from largest to smallest) are cement–tailing ratio, curing age, and slurry concentration. Additionally, the variation trend of backfill strength with these factors is clarified: (1) UCS decreases with the reduction in cement–sand ratio; (2) UCS increases steadily as slurry concentration rises; and (3) UCS increases significantly within the first 28 days of curing, while the strength growth rate slows down in the later stage.

Table 6. Range analysis results.

Factor	Uniaxial Compressive Strength (MPa)			Range
	Level 1	Level 2	Level 3	
A	2.119	0.953	0.618	1.501
B	0.880	1.221	1.489	0.609
C	0.855	1.259	1.576	0.721

ANOVA is conducted to verify the significance of each factor's effect on the backfill strength, with results summarized in Table 7. A significance level of $\alpha = 0.05$ is adopted, and the $F_{0.05}(2,2) = 19.0$ is obtained from the *F*-distribution table. The ANOVA results confirm that the cement–tailing ratio has the most significant impact on UCS, followed by curing age, while slurry concentration exerts the least obvious effect. Collectively, both range analysis and ANOVA demonstrate that the sensitivity of the three factors to the strength of granular-cemented backfill follows the order: cement–tailing ratio > curing age > slurry concentration.

Table 7. Variance analysis results.

Factor	Sum of Squares	Degree of Freedom	Mean Sum of Square	*F*-Value
A	4.528	2	2.264	37.094
B	1.225	2	0.613	11.920
C	2.125	2	1.063	23.330

7. Effects

From the results of cemented filling experiment of granular pile, the optimal slurry concentration suitable for on-site backfilling is determined to be 68%. At this concentration, a cement–tailing ratio ranging from 1:8 to 1:4 can meet the on-site strength requirements. Considering the potential existence of other illegal goafs at the bottom of the caving goaf, a cement–tailing ratio of 1:4 is adopted in the backfilling treatment.

The backfilling scheme was implemented on 22 October 2019. As of 23 September 2020, approximately 270,000 m^3 of slurry have been filled into the caving goaf of Shirengou Iron Mine, which quantitatively matched the initially detected goaf volume. However, observations from the −210 m level revealed that no backfill material was visible on the goaf floor, and the goaf remained in an active caving state. This indicates the presence of other illegal goafs connected to the lower part of the caving goaf. Due to the limitations of the current development and preparation status of Shirengou Iron Mine, the distribution range and volume of such illegal goafs cannot be detected. Therefore, the backfilling of the caving goaf must be continued at the −210 m level to simultaneously fill the other goafs connected to its lower part.

On 17 March 2021, all openings of the caving goaf at the −210 m level were blocked by caved loose rock piles. To observe the caving morphology of the goaf at this stage, a 3D laser scanner was used to perform 3D goaf scanning at the −180 m level. The measured goaf morphology is shown in Figure 19. At this time, the goaf floor remained inclined

southward, with a volume of 216,900 m^3, which was not significantly different from the 245,000 m^3 detected on 22 July 2019. As of 17 March 2021, the cumulative backfill slurry injected into the caving goaf reached 498,800 m^3, with the slurry concentration maintained at approximately 68%. However, the goaf volume remained at 216,900 m^3, indicating that all backfill slurry had infiltrated downward and the distribution range of the illegal goafs in the lower part of the caving goaf was far larger than the results of the previous 3D detection.

The schematic diagram of the right view changes from three goaf detections (Figure 22) shows that 18 months after the implementation of the backfilling scheme on 22 October 2019, the surrounding rock of the goaf below the −210 m level was effectively filled. The roof elevations measured in the three detections were −163.34 m, −152.54 m, and −129.32 m, respectively, with a maximum roof caving displacement of 34.02 m during this period. At this stage, due to the effective backfilling of the surrounding rock below the −210 m level, the possibility of large-scale caving of the caving goaf's surrounding rock was significantly reduced.

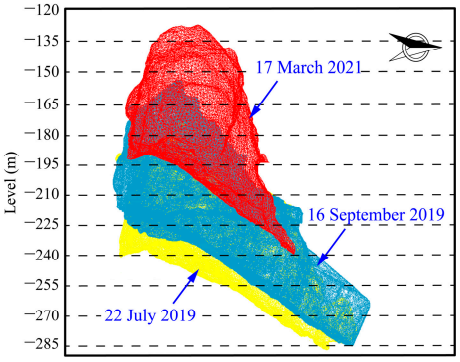


Figure 22. Changes in detection results for the right view of caving goaf. The scale bar is 1:1000.

The image results detected from the −180 m level (Figure 23) indicate that the goaf floor can be divided into a recently caving rock block area and a cemented filling area, confirming that all backfill slurry inside the caving goaf have infiltrated downward. Additionally, the distribution of rock blocks on the goaf floor shows that some areas clearly contain recently caved rock blocks, indicating occasional minor caving events with long intervals. This suggests that the caving goaf is basically in a stable state. In the subsequent backfilling and remediation process, the backfilling work will adopt the cemented backfilling instead of the waste rock-cemented backfilling.

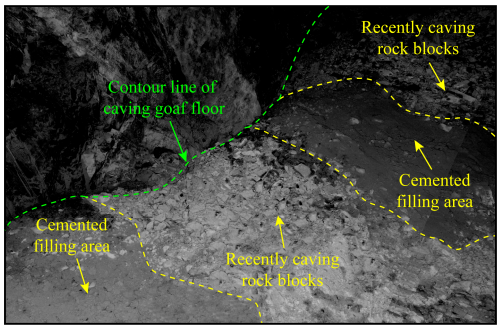


Figure 23. Image of the caving goaf floor on 17 March 2021.

8. Conclusions

Considering the engineering reality of "backfilling-while-caving" in the caving goaf of Shirengou Iron Mine, the physical similarity simulation experiment and uniaxial compres-

sive strength test were conducted to analyze the seepage law of backfill slurry in granular pile and the strength characteristics of granular-cemented backfill. Based on these analyses, the optimal mix ratio of backfill slurry suitable for the caving goaf was determined. From the above experiments, the following conclusions are drawn:

(1) Slurry concentration and the particle size of granular media exert a significant influence on the ease of seepage flow. The height of the granular piles determines the settlement zone of the slurry above the backfill, and the cement–tailing ratio has the least influence on the seepage and settlement of the backfill slurry.

(2) The critical concentration for the seepage of backfill slurry in the caving goaf of Shirengou Iron Mine is 68%. When the slurry concentration exceeds this critical value, a compacted slurry layer tends to form at the top of the granular pile, hindering the downward seepage of the remaining slurry. Conversely, when the concentration is lower than the critical value, lower slurry concentration facilitates easier seepage within the granular pile, but results in a larger settlement zone of the slurry above the backfill.

(3) The strength of the granular-cemented backfill is positively correlated with factors such as the cement–tailing ratio, curing age, and slurry concentration. Range analysis and analysis of variance (ANOVA) indicate that the cement–sand ratio has the highest sensitivity to backfill strength, followed by curing age, while slurry concentration exhibits the lowest sensitivity.

(4) When the backfill slurry with a cement–sand ratio of 1:8 to 1:4 is controlled at a concentration of 68%, it can achieve complete seepage and cementation of the granular pile layer. Under these conditions, the backfill strength reaches 1~2 MPa, which provides valuable guidance for the seepage and cementation of waste rock in the caving goaf of Shirengou Iron Mine.

Author Contributions: Z.D.: Conceptualization, methodology, software, and validation. J.Z.: Funding acquisition, formal analysis, writing—original draft. F.R. (Fuqiang Ren): Data curation, resources. F.R. (Fengyu Ren): Writing—review and editing. All authors have read and agreed to the published version of the manuscript.

Funding: The support of the Key Program of National Natural Science Foundation of China (Grant no. 52274113), the Youth Project of Yuman Province Basic Research Program (202401AU070175), and the Talent Introduction and Training Project of Kunming University of Science and Technology (No. KKZ3202421111) is gratefully acknowledged.

Data Availability Statement: The data used to support the findings of this study are included within the article.

Acknowledgments: The authors would like to thank the editors and the anonymous reviewers for their helpful and constructive comments.

Conflicts of Interest: Author Zhifu Dong was employed by the company Yunnan Gold Mining Group Co., Ltd. The remaining authors declare that the research was conducted in the absence of any commercial or financial relationships that could be construed as a potential conflict of interest.

References

1. Lv, C.; Lv, W.Y.; Sun, Q.; Xie, P.S.; Lang, D.; Ji, S.T.; Hu, J.J. Theoretical and technical concept of cemented backfill material for flexible enhanced thermal energy storage in coal underground space. *Chin. J. Coal Sci. Technol.* **2025**, *53*, 104–113.
2. Maest, A.S. Remining for renewable energy metals: A review of characterization needs, resource estimates, and potential environmental effects. *Minerals* **2023**, *13*, 1454. [CrossRef]
3. Cao, H.; Gao, Q.; Zhang, X.Z.; Guo, B. Research progress and development direction of filling cementing materials for filling mining in iron mines of China. *GELS* **2022**, *8*, 192. [CrossRef]

4. Zhang, J.Y.; Zhou, Z.H.; Zhang, J.; Liu, Y.; Liu, Y. Two-stage caving characteristics of complex irregular goaf: A case study in China. *Adv. Civ. Eng.* **2023**, *2023*, 7471721. [CrossRef]
5. He, R.X.; Zhang, J.; Liu, Y.; Song, D.; Ren, F. Determination of the ultimate underground mining depth considering the effect of granular rock and the range of surface caving. *Math. Probl. Eng.* **2021**, *2021*, 5576786. [CrossRef]
6. Zhou, N.; Ma, H.B.; Ouyang, S.Y.; Germain, D.; Hou, T. Influential factors in transportation and mechanical properties of aeolian sand-based cemented filling material. *Minerals* **2019**, *9*, 116. [CrossRef]
7. Fall, M.; Benzaazoua, M. Modeling the effect of sulphate on strength development of paste backfill and binder mixture optimization. *Cem. Concr. Res.* **2005**, *35*, 301–314. [CrossRef]
8. Huynh, L.; Beattie, D.A.; Fornasiero, D.; Ralston, J. Effect of polyphosphate and naphthalene sulfonate formaldehyde condensate on the rheological properties of dewatered tailings and cemented paste backfill. *Miner. Eng.* **2006**, *19*, 28–36. [CrossRef]
9. Ahmed, H.M.; Bharathan, B.; Kermani, M.; Hassani, F.; Hefni, M.A.; Ahmed, H.A.M.; Hassan, G.S.A.; Moustafa, E.B.; Saleem, H.A.; Sasmito, A.P. Evaluation of rheology measurements techniques for pressure loss in mine paste backfill transportation. *Minerals* **2022**, *12*, 678. [CrossRef]
10. Zhang, C.; Ma, C.; Chen, Q.; Liu, H.; Wu, S.; Pan, Z.; Zhang, L. Influence of rock percentage on strength and permeability of tailing-waste rock mixtures. *Bull. Eng. Geol. Environ.* **2020**, *80*, 399–411. [CrossRef]
11. Feng, F.; Xu, J.K.; Sun, S.H.; Cao, G.H. Research on mechanized vertical slicing and upward layered dry filling mining method for gently inclined thick and large ore bodies. *Chin. J. Met. Mine* **2024**, *10*, 1–5.
12. Vare, L.L.; Baker, M.C.; Howe, J.A.; Levin, L.A.; Neira, C.; Ramirez-Llodra, E.Z.; Reichelt-Brushett, A.; Rowden, A.A.; Shimmield, T.M.; Simpson, S.L.; et al. Scientific considerations for the assessment and management of mine tailings disposal in the deep sea. *Front. Mar. Sci.* **2018**, *5*, 17. [CrossRef]
13. Wang, C.; Dong, P.; Wang, Z.; Kong, P.; Yang, Y.; Zhou, Y.; Jiang, N. Case study on coal-based solid waste utilization in backfill paste: Hydration mechanism and performance analysis. *Case Stud. Constr. Mater.* **2025**, *22*, e04427. [CrossRef]
14. Bloss, M.L.; Greenwood, A.G. Cemented rock fill research at Mount Isa Mines limited 1992–1997. In Proceedings of the 6th International Symposium on Mining with Backfill, Brisbane, Australia, 14–16 April 1998; pp. 207–215.
15. Wang, Y.; Li, C.; Hou, Z.; Yi, X.; Wei, X. In vivo X-ray computed tomography investigations of crack damage volution of cemented waste rock backfills (CWRB) under uniaxial deformation. *Minerals* **2018**, *8*, 539. [CrossRef]
16. Wang, Y.; Xiao, Y.G.; Hou, Z.Q.; Li, C.H.; Wei, X.M. In situ X-ray computed tomography (CT) investigation of crack damage evolution for cemented paste backfill with marble waste block admixture under uniaxial deformation. *Arab. J. Geosci.* **2020**, *13*, 1018. [CrossRef]
17. Deb, D.; Sreenivas, T.; Dey, G.K.; Panchal, S. Paste backfill technology: Essential characteristics and assessment of its application for mill rejects of uranium ores. *Trans. Indian Inst. Met.* **2017**, *70*, 487–495. [CrossRef]
18. Zhang, D.; Hao, Y.; Wen, H.; Sun, W.; Zhai, X. Properties optimization and hydration mechanism of coal-based solid waste paste filling materials. *Powder Technol.* **2025**, *455*, 120751. [CrossRef]
19. Ren, F.Y.; Yang, L.; Zhang, D.J.; He, R.X.; Zhou, Y.J. Discussion on the treatment schemes of goaf closing to the main shaft in fluorite mine. *Chin. J. Min. Res. Dev.* **2017**, *37*, 21–25.
20. He, B.Q.; Jian, W.B. Filling super-large goaf with solid waste under large-scale mechanized operation. *Chin. J. Met. Mine* **2019**, *7*, 19–25.
21. Yan, R.; Yin, S.; Zhang, H.; Wang, L.; Chen, D. Effect of superplasticizer on the setting behaviors and mechanical properties of tailings-waste rock cemented paste backfills. *Case Stud. Constr. Mater.* **2023**, *18*, e01714. [CrossRef]
22. Jin, J.; Liu, T.; Li, M.; Lv, T.; Zhang, S.; Zuo, S. Mechanical properties and compression damage characteristics of coal gangue-filled backfill cemented by fly ash modified self-consolidating grouts. *Case Stud. Constr. Mater.* **2025**, *22*, 04687. [CrossRef]
23. Qiu, J.H.; Xiong, X.; Zhou, K.P. Fractal characterization and NMR analysis of curing-dependent pore structures in cemented tailings waste rockbackfill. *Fractal Fract.* **2025**, *9*, 367. [CrossRef]
24. Gao, T.; Wu, A.; Wang, S.; Ruan, Z.; Chen, C.; Sun, W. Experimental and numerical investigations of bending mechanical properties and fracture characteristics of cemented tailings-waste rock backfill under three-point bending. *Constr. Build. Mater.* **2024**, *447*, 138149. [CrossRef]
25. Gao, B.; Cao, S.; Yilmaz, E. Effect of content and length of polypropylene fibers on strength and microstructure of cementitious tailings-waste rock Fill. *Minerals* **2023**, *13*, 142. [CrossRef]
26. Chen, G.; Yao, N.; Ye, Y.; Fu, F.; Hu, N.; Zhang, Z. Study on mechanical properties and damage characteristics of cemented waste rock-tailing backfill. *Environ. Sci. Pollut. Res.* **2023**, *30*, 102181–102197. [CrossRef]
27. Sun, Q.; Li, B.; Wang, Y.; Wang, H. Durability and life prediction of fly ash geopolymer concrete in corrosion environments caused by dry and wet circulation. *Environ. Sci. Pollut. Res.* **2022**, *29*, 39743–39753. [CrossRef]
28. Xu, W.B.; Chen, W.; Zhang, Y.L.; Chen, B. Research on rheological characteristics of gangue-fly ash slurry in deep filling mining. *Chin. J. Coal Sci. Technol.* **2023**, *51*, 85–93.

29. Hu, C.Y.; Mei, F.D.; Liu, X.Q.; Wang, G.D.; Zhang, F.H. Influence of exposure time on stability of the Gangli Iron Mine caved stope considering creep effects. *Chin. J. Saf. Environ. Eng.* **2025**, *32*, 113–127.
30. Xiang, H.W.; Lu, Y.Z.; Liu, Z.Y.; Wang, S.G.; Wang, L.J. Influence of pillars in drifting chamber on roof stability during sublevel open stoping with backfill. *Chin. J. Min. Metall. Eng.* **2025**, *45*, 69–76.
31. Li, H.; Shi, M.; Zhang, J.; Peng, L. An experimental study on the influence of low—Cement content on improved filling characteristics of geotextile bags filled with fine tailings slurry. *Front. Mar. Sci.* **2025**, *12*, 1529905. [CrossRef]
32. Tu, B.; He, H.; Liu, L.; Ding, X.; Yang, Q. Comparative analysis of uniaxial and triaxial compression characteristics of cement tailings backfill. *Min. Metall. Explor.* **2025**, *42*, 335–345. [CrossRef]
33. Ma, K.; Yang, T.; Zhao, Y.; Liu, H.; Dong, X.; Gao, Y.; Liu, Y.; Li, J.; He, R.; Hou, J. Study on the Distribution Laws of Lateral Force Induced by the Drawing Ore and Orebody Dip. *Chin. J. Met. Mine* **2021**, *8*, 57–60.
34. Ren, F.Y.; Liu, Y.; He, R.X.; Zhang, J. Flow-through features of tailings in subsidence area under ore drawing conditions. *Chin. J. Northeast. Univ.* **2020**, *41*, 858–887.

Disclaimer/Publisher's Note: The statements, opinions and data contained in all publications are solely those of the individual author(s) and contributor(s) and not of MDPI and/or the editor(s). MDPI and/or the editor(s) disclaim responsibility for any injury to people or property resulting from any ideas, methods, instructions or products referred to in the content.